Available online at www.sciencedirect.com
SCIENCE DIRECT®

Journal of the European Ceramic Society 24 (2004) 979–984

www.elsevier.com/locate/jeurceramsoc

PLD of perovskite coatings for optoelectronics, microelectronics, and microtechnology

E.W. Kreutz*, J. Gottmann

Lehrstuhl für Lasertechnik, RWTH Aachen, Steinbachstr. 15, 52074 Aachen, Germany

Abstract

The deposition of $BaTiO_3$ thin films by pulsed excimer laser radiation (248 nm) on Pt/Ti/Si(111) and Pt/Ti/Si(100) substrates is investigated as a function of the processing variables laser fluence, processing gas pressure and target-to-substrate distance. The influence of the kinetic energy of the film-forming particles on the crystalline structure, defects and orientation and on the resulting electrical properties of the films is investigated. X-ray diffraction measurements and polarisation-dependent micro Raman measurements reveal a *c*-axis orientation normal to the substrate surface, in the case of high particle energy (> 50 eV), while at low kinetic energies (<30 eV) a $[111]_{pc}$ or $[110]_{pc}$ orientation is preferred. The ferroelectricity and the dielectric constant of the films, determined by impedance measurements, decrease with increasing kinetic energy of the film-forming particles from $\varepsilon_r = 1000$–2200 to $\varepsilon_r = 200$–700. This decrease correlates with the change of the orientation and with an increasing lattice constant of the films, indicating that particles with high kinetic energies produce crystal defects and stress in the growing film.

Keywords: $BaTiO_3$; Crystalline orientation; Ferroelectric properties; Films; Pulsed laser deposition; X-ray methods

1. Introduction

The development of low-cost composite-substrate integrated optical components that can generate, amplify or modulate light would enhance the capabilities of long-distance communication systems, local area networks, and chip-to-chip interconnects. The integration of electro-optical devices like waveguide phase modulators for switches based on ferroelectric $BaTiO_3$ is one of several strategies toward the realization of this type of opto-electronic integrated circuits, which has been demonstrated using pulsed laser deposition for the thin film preparation on MgO single crystals and ion beam etching for the fabrication of Mach-Zehnder optical waveguide modulators.[1]

Among other vapour deposition techniques such as thermal evaporation, sputtering, chemical vapour deposition, molecular beam epitaxy, ion beam deposition or electron beam evaporation,[2] pulsed laser deposition (PLD)[3] plays a major role because of the wide range of target materials which can be removed stoichiometrically, and due to the flexibility in choosing type and pressure of a processing gas. During PLD high-energy excited species in the vapour/plasma plume are produced, which can be decelerated and can react by interaction with the processing gas particles,[4] resulting in various structural film properties at moderate substrate temperatures, depending on the laser parameters and processing variables used.

To optimise the growth of thin films with desired properties for applications, an understanding of the different physical processes, especially the dynamics of the laser-induced vapour/plasma and its dependence on the processing variables, is necessary. The main emphasis of the experimental investigations is to investigate the effect of the kinetic energy of the film-forming particles on the structural and electrical properties of the deposited $BaTiO_3$ films.

2. Experiment

2.1. Pulsed laser deposition

A KrF excimer laser (wavelength $\lambda_L = 248$ nm, pulse duration $\tau_L = 20$ ns (FWHM), pulse energy $E_L < 400$ mJ,

* Corresponding author. Tel.: +49-241-8906-146; fax: +49-241-8906-121.
E-mail address: kreutz@llt.rwth-aachen.de (E.W. Kreutz).

0955-2219/$ - see front matter © 2003 Elsevier Ltd. All rights reserved.
doi:10.1016/S0955-2219(03)00514-4

repetition rate $\nu_{rep} < 400$ Hz) is used for PLD. The laser radiation is formed by a mask, which is imaged by a telescopic lens system to a rectangular cross-section of $A_L = 1.2 \times 1.8$ mm^2 with sharp edges on the target surface at an angle of incidence of 45°.[5] Laser fluences up to $\varepsilon_L = 4.8$ J/cm^2 are achieved on the target surface. As processing gas oxygen at pressures of $p = 10^{-2}$- 100 Pa is used. The base pressure of the vacuum system is 10^{-4} Pa. The heatable substrate is positioned at a distance of $d = 2$–5 cm from the sintered $BaTiO_3$ target at an angle of 45° between target normal and substrate normal.[5] Deposition rates between 0.04 nm/pulse (fluence $\varepsilon_L = 3.2$ J/cm^2, target-to-substrate distance $d = 4$ cm) and 0.15 nm/pulse ($\varepsilon_L = 4.8$ J/cm^2, $d = 2.6$ cm) are achieved. Si(100) and Si(111) wafers, coated by dc sputtering with a 20 nm Ti adhesion layer and a 100 nm Pt bottom electrode, are used as substrates. The $BaTiO_3$ films 200 nm in thickness were deposited at substrate temperatures of 500–700 °C, measured by pyrometry of the virgin platinum surface of the substrates prior to deposition or of the rough heater surface during deposition. After film deposition Pt top electrodes (diameter 500 μm, thickness 100 nm) are deposited by dc sputtering.

2.2. Film diagnosis tools

Film thickness and refractive index are determined ex-situ by single-wavelength ($\lambda = 633$ nm) ellipsometry, fitting calculated Ψ-Δ values to data of line-scans across the films with an inhomogeneous thickness distribution.[6]

The dielectric and ferroelectric properties of the $BaTiO_3$ films are determined from impedance measurements using a modified Sawyer–Tower circuit by applying a maximum electric field strength of 400 kV/cm with a frequency of 10 kHz to the films.[7] The dielectric constant ε_r was defined as the slope of the resulting hysteresis at $E = 0$.

Structural characterisation of the films is carried out with polarisation dependent micro Raman spectroscopy and X-ray diffraction (θ–2θ scans in Bragg–Brentano geometry) using the CuK_α ($\lambda_? = 0.15406$ nm) and CuK_α ($\lambda = 0.15444$ nm) radiation without monochromator. The Raman spectra are excited by a 500 mW Ar-ion laser operating at a wavelength of $\lambda = 488$ nm. The exciting laser radiation is directed onto the sample via a microscope optics, corresponding to back-scattering geometry (z-axis parallel to sample normal) mixed with forward scattering due to reflection at the Pt bottom electrode. Polarisation-dependent measurements were carried out either with incident and measured polarisation parallel ($-z(xx)z$ geometry) or orthogonal ($-z(xy)z$ geometry) to each other. To avoid sample heating by the Ar-ion laser radiation above $T_C = 120$ °C, where $BaTiO_3$ becomes paraelectric, a maximum power of 5 mW on the sample is used, leading to a temperature of 80 °C in the sample as determined by Stokes/Anti-Stokes measurements. The back-scattered light is dispersed in a triple monochromator and detected with a cooled Si diode array.[8]

3. Results and discussion

3.1. Texture of the films by XRD

No tetragonal distortion is observable in the investigated $BaTiO_3$ films 200 nm in thickness, which may be associated with the small grain size of the films and which is also due to the use of a non-monochromatic X-ray source. Therefore, in the following only pseudocubic textures are reported until the orientation of the films is revealed by Raman spectroscopy. XRD results reveal pure polycrystalline $BaTiO_3$ phase of the films.

The intensities of the XRD peaks of the $BaTiO_3$ films relative to the pseudo cubic peak intensities of a powder sample were normalised for comparison to $I([100]_{pc}) + I([110]_{pc}) + I([111]_{pc}) = 100$.

Films deposited at $T_{Sub} = 550$ °C on Pt/Ti/Si(100) substrates show a predominant $[100]_{pc}$ texture when using low processing gas pressures of p = 2–5 Pa and a mixed $[110]_{pc}$ and $[111]_{pc}$ texture at $p = 10$–20 Pa (Fig. 1). Increasing the substrate temperature from $T_{Sub} = 550$ °C to $T_{Sub} = 600$ °C and $T_{Sub} = 700$ at $p = 20$ Pa causes the texture of films to change less than 10%.

The changes in the evolving film texture may be explained by the increase of kinetic energy of the film-forming particles with decreasing processing gas pressure.[9,10] The possible physical mechanisms responsible for this effect include orientation dependent etching by momentum transfer of kinetic particles and the nucleation of oriented crystallites during thermal spikes. Thermal spikes are generated, if the energy of kinetic particles thermalizes in a few top monolayers during the growth of the film. The surface of the Pt(111) electrode,

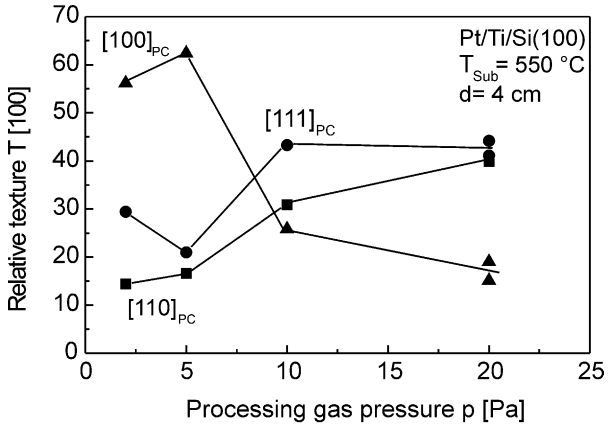

Fig. 1. Texture of $BaTiO_3$ films deposited at $T_{Sub} = 550$ °C, $d = 4$ cm, $\varepsilon_L = 3.2$ J/cm^2 on Pt/Ti/Si(100) substrates, determined by XRD.

which forms on Si(100),[11] Ti/Si(100) and predominantly also on Ti/Si(111),[12] may be penetrated and disturbed by film-forming particles impinging with high kinetic energies on the Pt surface during the beginning of the film growth. On the modified Pt surface the nucleation of $[100]_{pc}$ $BaTiO_3$ crystallites may be favoured. The heteroepitaxial growth of $BaTiO_3(111)$ on Pt(111)[13] is then possible, if the kinetic energy of the film-forming particles is neither sufficient to rearrange the Pt(111) surface nor to cause crystal defects in the growing $BaTiO_3$ film.

The texture of films deposited at $T_{Sub} = 600$ °C on Pt/Ti/Si(111) changes from predominantly $[110]_{pc}$ to predominantly $[111]_{pc}$ with increasing processing gas pressure (Fig. 2).

Increasing the substrate temperature to $T_{Sub} = 700$ °C causes the films to grow with predominant $[100]_{pc}$ texture at $p = 1.3$ Pa and $p = 20$ Pa.[14] The change of the texture from predominantly $[111]_{pc}$ to predominantly $[100]_{pc}$ with increasing substrate temperature leads to the conclusion that the growth of $[100]_{pc}$ orientated $BaTiO_3$ could be heteroepitaxially on the used Pt/Ti/Si(111) substrates because the minimisation of the free surface energy is crucial for the formation of small crystallites. Although, heteroepitaxial growth of $BaTiO_3(111)$ on the formed Pt(111) layer seems to be more natural.[13] At lower temperatures and kinetic energies the developing $[111]_{pc}$ orientation may also originate from the growth of the crystallites in the direction of the incident particle flux allowing preferential growth due to a limited diffusion length.

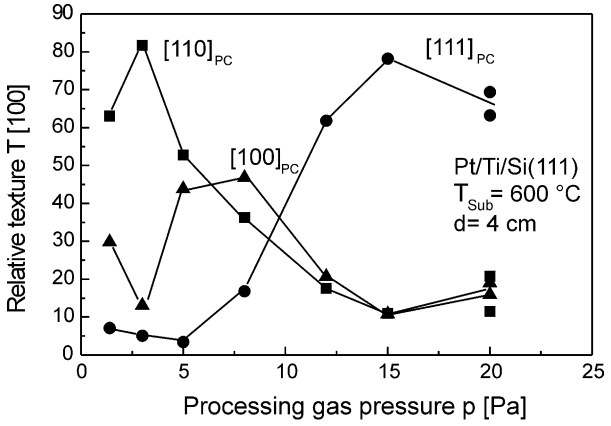

Fig. 2. Texture of $BaTiO_3$ films deposited at $T_{Sub} = 600$ °C, $d = 4$ cm, $\varepsilon_L = 3.6$ J/cm^2 on Pt/Ti/Si(111) substrates, determined by XRD.

Following scanning electron microscopy (Fig. 3) the surfaces of [100] films appear smother than the [111] ones showing irregularly distributed cubes with its [111] orientation directed away from the film surface.

The lattice constant of the $BaTiO_3$ films, as determined from the peak positions of the $(100)_{pc}$, $(110)_{pc}$ and $(111)_{pc}$ peaks of the X-ray diffraction spectra by averaging, decreases with increasing processing gas pressure from 0.404 to 0.399 nm (Fig. 4). The decrease of the lattice constant with increasing processing gas pressure and increasing target-to-substrate distance can not be explained alone by the changes in the texture[15] but with a decreasing amount of oxygen vacancies in the films.[16] With decreasing processing gas pressure the kinetic energy of the film-forming particles increases.[9,10] Above a threshold (around 20–50 eV) hyperthermal particles impinging on the growing surface generate defects beneath the surface layer via momentum transfer,[17] thus resulting in a larger amount of oxygen vacancies in the films.

3.2. Orientation of the films by Raman spectroscopy

Raman spectra of $BaTiO_3$ films with a preferential $[100]_{pc}$ ($T_{Sub} = 550$ °C, $p = 5$ Pa, $d = 2.6$ cm, $\varepsilon_L = 4.8$ J/

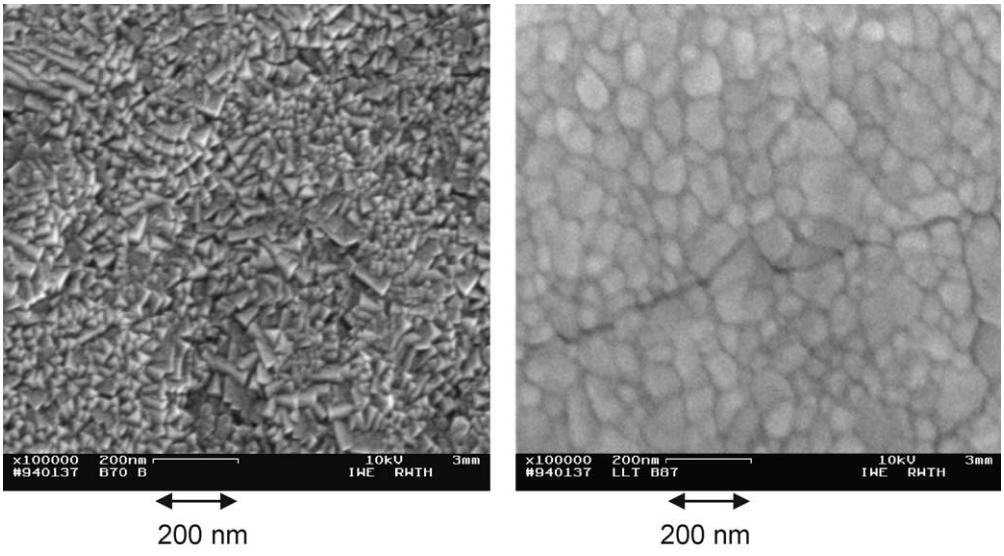

Fig. 3. Top view of $BaTiO_3$ films with $[111]_{PC}$ texture (left) and $[100]_{PC}$ texture (right) as measured by SEM.

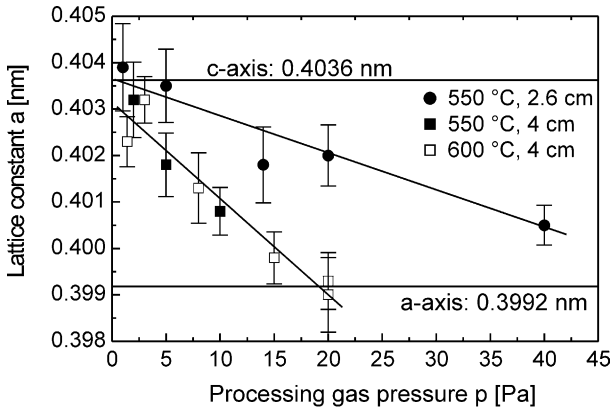

Fig. 4. Lattice constant of $BaTiO_3$ films versus processing gas pressure for different target-to-substrate distances and substrate temperatures.

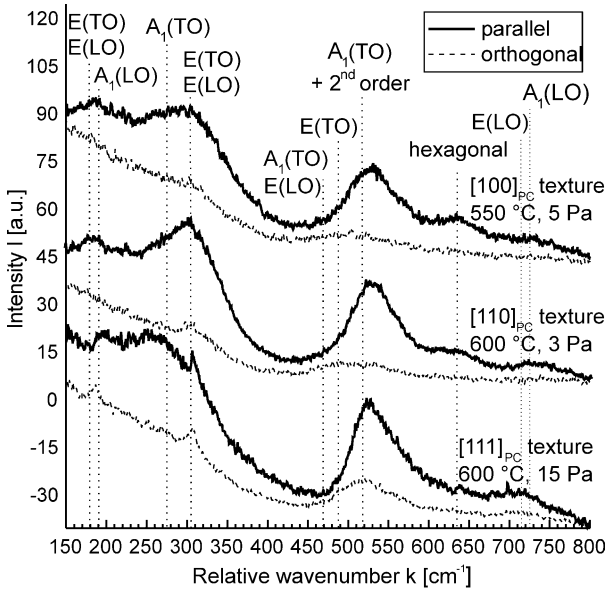

Fig. 5. Raman spectra of $BaTiO_3$ films, deposited with different preferential textures on Pt/Ti/Si(111) substrates; Raman scattering geometry was parallel$-z(xx)z$ and orthogonal $-z(xy)z$, respectively.

cm^2), $[110]_{pc}$ ($T_{Sub}=600$ °C, $p=3$ Pa, d = 4 cm, $\varepsilon_L=3.6$ J/cm^2) and $[111]_{pc}$ texture ($T_{Sub}=600$ °C, $p=15$ Pa, $d=4$ cm, $\varepsilon_L=3.6$ J/cm^2) deposited on Pt/Ti/Si(111) substrates were recorded both with parallel ($-z(xx)z$) and orthogonal ($-z(xy)z$) scattering geometry, to distinguish between the phonons with E symmetry, which are allowed in (xx) and (xy) geometry, and the phonons with A_1 symmetry, which are forbidden in (xy) geometry.[18]

By comparing the Raman peaks (Fig. 5) with the Raman-active phonons in tetragonal $BaTiO_3$ (Table 1) it is concluded, that the film with $[100]_{pc}$ texture exhibits mean c-axis orientation (wave vector and c-axis are parallel, θ = 0°): The peak at 730 cm^{-1} is visible in parallel (xx) and not in orthogonal (xy) geometry and has been therefore identified as A_1(LO), which is only measurable if the c-axis is parallel to the direction of exciting laser radiation. The appearance of the A_1(LO) phonon at 191 cm^{-1} and the missing A_1(TO) at 275 cm^{-1} are sustaining this assumption. A slight shift of the phonons to higher wavenumbers may be the result of compressive stress in the film or of worse crystallinity, as also indicated by the XRD measurements. At 635 cm^{-1} a phonon corresponding to the A_{1g}(LO) band of metastable hexagonal $BaTiO_3$ impurities is observed, which may be formed during the rapid cooling following thermal spikes developing during deposition under the energetic particle bombardment.[19] The hexagonal phase is not observed using XRD, possibly due to the short order of this localised impurities. The large width of the peak at 306 cm^{-1} may be due to crystal defects like oxygen vacancies produced by momentum transfer from energetic particles impinging on the surface during the growth. In the film with $[111]_{pc}$ texture a phonon at 720 cm^{-1} is visible in the (xy) geometry, therefore the symmetry of this phonon is at least partly E(LO). The A_1(TO) phonon at 275 cm^{-1} is mixed with the E(TO) phonon at 37 cm^{-1} and therefore shifted to around 260 cm^{-1}, corresponding to an angle between the surface normal and the polar c-axis of θ = 60–75°.[20] Therefore the main component of the polar c-axis vector is within the substrate plane.

The bands around 520 cm^{-1} in the (xy) spectra are due to backscattering from the TO phonons and higher order processes.[18]

3.3. Electrical properties of the films

The dielectric constant of films 200 nm in thickness deposited at $T_{Sub}=550$ °C, $d=2.6$ cm and $\varepsilon_L=4.8$ J/cm^2 increases with the processing gas pressure, while the dielectric constant of films deposited at $T_{Sub}=550$ °C, $d=4$ cm and $\varepsilon_L=3.6$ J/cm^2 shows a maximum of $\varepsilon_r=1000$–1300 at p = 10–20 Pa (Fig. 6). The dielectric

Table 1
Raman-active phonons in tetragonal $BaTiO_3$ for phonons with their wave vector parallel ($\theta=0°$) and normal to the polar c-axis ($\theta=90°$). For oblique phonons the modes mix and the frequencies are between the given values.[20]

Symmetry ($\theta=0°$)	E(TO)	E(TO)	A_1(LO)	E(TO)	A_1(TO)	E(TO)	A_1(LO)
Frequency [cm^{-1}]	37	181	191	306	471	487	725
Symmetry($\theta=90°$)	A_1(TO)	E(LO)	A_1(TO)	E(LO)	E(LO)	A_1(TO)	E(LO)
Frequency [cm^{-1}]	175	180	275	305	468	516	717

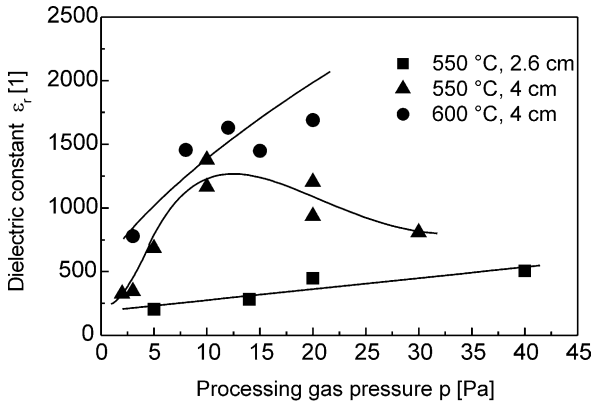

Fig. 6. Dielectric constant of $BaTiO_3$ films versus processing gas pressure.

constant of films deposited at $T_{Sub} = 600$ °C, $d = 4$ cm and $\varepsilon_L = 3.6$ J/cm^2 increases with the processing gas pressure to $\varepsilon_r = 1600$–2200.

The films showing a low dielectric constant of $\varepsilon_r = 200$–700 are the $[100]_{pc}$ textured films with c-axis orientation, as revealed by XRD measurements and Raman spectroscopy, respectively, and are grown using low processing gas pressures and/or low target-to-substrate distances, correlating with high kinetic energies of the film-forming particles $E_{kin} > 80$ eV. The films with high dielectric constant of $\varepsilon_r = 1000$–2200 are $[110]_{pc}$ or $[111]_{pc}$ textured with the main component of their polar *c*-axis within the substrate plane ($\theta = 60$–$75°$), which is necessary for the high dielectric constant,[21] indicating a lower oxygen vacancy density and a larger crystallite size, caused by enhanced diffusion. These films are deposited using kinetic energies of the film-forming particles in the range of 10–30 eV, which generate no bulk displacements in the growing films but enhance the diffusion of surface atoms.[17]

4. Conclusion

The kinetic energy of the film-forming Ba particles, as determined by time-of-flight quadrupole mass spectrometry, is governed by the processing parameters target-to-substrate distance, fluence and processing gas pressure and can be controlled in a wide range between 2 and 200 eV. The kinetic energy of the film-forming particles increases with the fluence and decreases with the processing gas pressure and the target-to-substrate distance.

The structural characteristics of the deposited $BaTiO_3$ thin films are governed by the orientation of the used substrate, the substrate temperature during deposition and the kinetic energy of the film-forming particles. Preferred *c*-axis oriented films are obtained using particles with high kinetic energies and a Pt/Ti/Si(100) substrate or high temperatures ($T_{Sub} = 700$ °C) and Pt/Ti/Si(111) substrates. Preferred $[110]_{pc}$ oriented films grow at 600 °C on Pt/Ti/Si(111) substrates using high kinetic energies. A predominantly $[111]_{pc}$ texture is obtained using low kinetic energies of the film-forming particles. The main component of the polar c-axis of the predominant $[111]_{pc}$ textured films is within the substrate plane with an angle of $\theta = 60$–$75°$ between the *c*-axis and the substrate normal, as determined by Raman spectroscopy.

The electrical properties of the films are related to their structural properties. $BaTiO_3$ films with mainly $[111]_{pc}$ texture and a high component of the polar *c*-axis within the substrate plane show the highest dielectric constant of $\varepsilon_r = 1000$–2200, increasing with the substrate temperature from 550 to 700 °C. Films with predominant $[100]_{pc}$ texture and *c*-axis orientation exhibit a dielectric constant of $\varepsilon_r = 200$–700, increasing with the substrate temperature, too.

Acknowledgements

The authors thank U. Hasenkox (IWE II, RWTH Aachen) for assistance in XRD-measurements.

References

1. Petraru, A., Siegert, M., Schmid, M., Schubert, J. and Buchal, Ch., Ferroelectric $BaTiO_3$ thin film optical waveguide modulators, *Mater. Res. Soc. Symp. Proc. 688* (*Ferroelectric Thin Films X, 2001)*, in press.
2. Ohring, M., *The Materials Science of Thin Films*. Academic Press, San Diego, 1992.
3. Chrisey, D. B., Hubler, G. K., ed., *Pulsed Laser Deposition of Thin Films*. John Wiley & Sons, New York, Chichester, Brisbane, Toronto, Singapore, 1994.
4. Catherinot, A., Angleraud, B., Auberton, J., Champaux, C., Germain, C. and Girault, C., *Surface Treatment and Film Deposition*. NATO ASI, 1994.
5. Gottmann, J. and Kreutz, E. W., *Surf. Coat. Technol.*, 1999, **116-119**, 1189.
6. Tompkins, H. G., *A Users's Guide to Ellipsometry*. Academic Press, San Diego, 1993.
7. Sawyer, C. B. and Tower, H. C., *Phys. Rev.*, 1930, **35**, 269.
8. Klotzbücher, T., Mergens, M., Husmann, A., Gottmann, J. and Kreutz, E. W., in ALT'97 International Conference on Laser Surface Processing, V.I. Pustovoy, Editor, Proceedings of SPIE 3404, 323 (1998).
9. Gottmann, J., Klotzbücher, T. and Kreutz, E. W., in ALT'97 International Conference on Laser Surface Processing, V.I. Pustovoy, Editor, Proceedings of SPIE 3404, 8 (1998).
10. Gottmann, J. and Kreutz, E. W., *Appl. Phys. A*, 2000, **70**, 275.
11. Hayasi, T., Ohji, N., Hirohara, K., Fukunaga, T. and Maiwa, H., *Jpn. J. Appl. Phys.*, 1993, **33**, 4092.
12. Mertin, M., Offenberg, D., An, C. W., Wesner, D. A. and Kreutz, E. W., *Appl. Surf. Sci.*, 1996, **96-98**, 842.
13. Iijima, K., Terashima, T., Yamamoto, K., Hirata, K. and Bando, Y., *Appl. Phys. Lett.*, 1990, **56**, 527.
14. Gottmann, J., Klotzbücher, T., Vosseler, B. and Kreutz, E. W., *Mater. Res. Soc. Symp. Proc.*, 1998, **526**, 175.

15. Börnstein, Landolt., *Crystal and Solid State Physics, New Series, Ferroelectrics and Related Substances, Subvolume a: Oxides (28), III*. Springer Verlag, Berlin, Heidelberg, New York, 1989.
16. Schenk, P. K., Vaudin, M. D., Lee, B. W., Bonnel, D. W., Hastie, J. W. and Paul, A. J., *Mater. Res. Soc. Symp. Proc.*, 1995, **361**, 527.
17. Brice, D. K., Tsao, J. Y. and Picraux, S. T., *Nucl. Instr. Meth. Phys. B*, 1989, **44**, 68.
18. Scalabrin, A., Chaves, A. S., Shim, D. S. and Porto, S. P. S., *Phys. Stat. Sol. (b)*, 1977, **79**, 731.
19. Alexander, D. E. and Was, G. S., *Mater. Res. Soc. Symp. Proc*, 1991, **202**, 205.
20. Nakamura, T., *Ferroelectrics*, 1992, **137**, 65.
21. Moulson, A. J. and Herbert, J. M., *Electroceramics: Material Properties Applications*. Chapman & Hall, London, New York, Tokyo, Melburne, Madras, 1990.